

Mineralogy Classification Comparison to Empirical Log Relationship and Implication for Physics Informed Machine Learning

David J. Emery, Marcelo Guarido, and Daniel O. Trad
University of Calgary, CREWES

Summary

Machine Learning has given us a new way of investigating the petrophysical and seismic relationship with lithology, porosity and pore fluid. This poster displays our analysis of over 300 wells with DT, Shear & RHOB logs from the North Sea, New Zealand, Australia, and Canada. The learning data used for this analysis is from the FORCE2020 Lithology Prediction Contest reworked into 18 mineral categories. As a consequence, we are better able to understand log relationships with mineralogy along with estimating missing sonic, shear and density logs than using the standard empirical relationships.

Introduction

The regression method (Faust, 1951; Faust, 1953; Gardner, Garner, & Greogory, 1974; Castagna, Batzle, & Eastwood, 1985) became the standard method for creating missing logs. These empirical relationships worked well for post-stack interpretation (Tanner & Sheriff, 1977; Brown, 1999) and inversion (Lindseth, 1976; Aki & Richards, 1980; Ostrander, 1984; Shuey, 1985; Russell & Hampson, 1991; Castagna, Batzle, & Kan, 1993). The adoption of AVO analysis (Russell B., Hampson, Schuelke, & Quirein, 1997; Goodway, Chen, & Downton, 1997; Connolly, 1998) during the late '90s started to emphasize several shortcomings of these basic estimations. Applying rock physics standards (Mavko, Mukerji, & Dvorkin, 1998; Avseth & Odegaard, 2004; Emery & Steward, 2006; Lee, 2006; Russell & Lines, 2013) has significantly improved geophysical interpretation, providing knowledge of lithology and fluid types are known before estimating missing velocity and density information.

Machine Learning has recently become popular in petrophysics, with multiple publications outlining its uses in lithology prediction (Hall B. , 2016; Hall & Hall, 2017; Guarido, 2019; Emery D. J., Guarido, Trad, & Innanen, 2021). Regrettably, most of these solutions require complete log data. The primary Machine Learning difficulties consist of the ill-conditioning of well logs, uneven sampling, finding the correct features engineering solutions, the need to impute missing values and overfitting.

This poster focuses on showing the petrophysical, rock physic, and AVO cross plots for common mineralogy, the application of these results in the estimation of mineral classes and, the potential match to rock lab-derived properties.

Theory

The more common methods for estimating V_p , V_s and RHOB are based in physics-based from rock lab-derived modulus (Mavko 1988; Dvorkin & Nur 1996), V_p/V_s vs I_p (Avseth & Ødegaard, 2004; Avseth et al. 2009 & 2010) or from Lambda-Rho/Mu-Rho relationships (Goodway 1997 & 2001, Hoffe et al. 2008).

Estimating V_p & V_s assuming an isotropic rock can be derived from the bulk modulus (K), shear modulus (μ) and density (ρ) using:

$$V_p = \sqrt{\frac{k + 4/3\mu}{\rho}} \quad \text{and} \quad V_s = \sqrt{\frac{\mu}{\rho}} \quad (1)$$

To estimate V_p & V_s , the first one needs to determine the mineral values for K and ρ , and then estimate the variation in values with porosity. This variation with porosity generally requires estimating using a combination of a soft (Reuss lower) or hard (Voigt upper) estimation.

Density (ρ) generally follows a Voigt averaging, while bulk (K) & shear moduli (μ) generally lie between the bounds. Various averaging technics such as Voigt-Reuss-Hill, Hashin-Shtrikman, or Kuster-Toksoz, along with the more popular Gassmann's formulation, have been proposed. Nur proposed (Mavko, 1998) a more physical basis for associating a rock's mineralogy to its log properties by assuming that the bulk and shear modulus are equivalent to the mineral grains at extremely low porosities and the Reuss bound when the rock loses cohesion (Φ_c critical porosity).

The isotropic formulas for deriving moduli's from V_p , V_s and density (ρ) are:

$$K = \rho(V_p^2 - 4/3 V_s^2) \quad \mu = \rho V_s^2 \quad (2)$$

Likewise, the Poisson's ratio can be derived using V_p and V_s by:

$$\sigma = \frac{V_p^2 - 2V_s^2}{2(V_p^2 - 2V_s^2)} \quad (3)$$

Another rock-physics model involves cross-plotting of V_p/V_s versus $\ln \rho$, which is relatively straightforward using petrophysical logs. The final common cross-plot we use for evaluating V_p , V_s and density is the Lambda-Rho ($\lambda\rho$) Mu-Rho Rho ($\mu\rho$) variation in lithology and fluids (Goodway 1997 & 2001, Hoffe et al. 2008). The formulas used for estimating Lambda-Rho (λ) and Mu-Rho (μ) are:

$$\lambda = \rho(V_p^2 - 2V_s^2) \quad \mu = \rho V_s^2 \quad (4)$$

Most of these empirical relationships, along with the rock-physics formulation, are for siliciclastic rocks at reservoir depths, temperatures, and pressure. As the petrophysical logs used for the Machine Learning solution in this report vary from near the water bottom to over 5000 meters below the sea floor, some variation is expected. The input mineralogy is dominantly siliciclastic (88%), with shale making up 72% of the overall, thus providing a reasonable background trend that we can use to normalize data between wells and derive mineralogical relationships. Figure 1, shows the complete dataset, the derived trends from the linear normalization, and the location of some of the mineralogy.

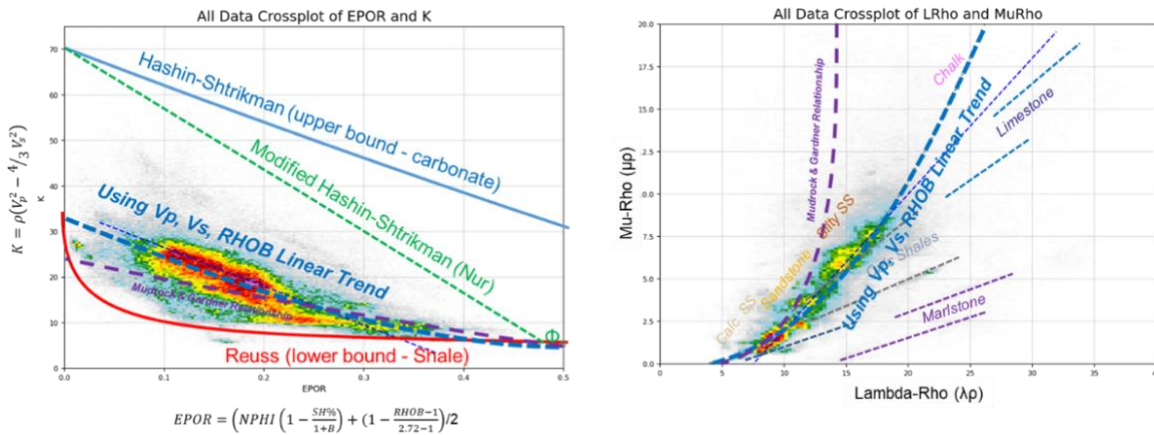


Figure 1: Bulk Modulus (left) and Lambda-Rho/Mu-Rho (right) cross plots of input data

Results

We were fortunate to be provided with a petrophysical analysis for a learning dataset of 118 wells (FORCE 2020) and these wells provide a framework for the estimation of mineralogy for the remaining wells within the dataset. Figure 2 shows the V_p , V_s , V_p/V_s , and RHOB cross-plot against depth after normalization for the complete dataset. While a logarithm relationship would be expected, our analysis indicated using a simpler linear estimate was more stable. While we believe there are potentially multiple geological reasons for not seeing the expected logarithm decay with depth, we believe the lack of sufficient shallow well information is the predominant factor. Deviation from this linear trend appears to be predominately along diagenetic variation with the conversion of smectite to illite and opal-A & CT to quartz being the most significant.

Earlier work (Emery et al., 2021 & 2022) showed that removing this linear trend before performing machine learning estimation for mineralogy significantly improves results. The predominant factor effecting by this correlation is changes in porosity caused by compaction and the residual porosity changes are dominantly the results in mineralogy. Using the linear relationship works well when converting the petrophysical logs (figure 1) into rock physic/engineering space (bulk modulus (K), shear modulus (μ), Poisson's ratio (σ), and seismic cross-plots (V_p/V_s vs I_p , LMrho).

This poster demonstrates the advantage of using machine learning as we can show more than a simple three mineral classes (quartz-SS, clay-SH, & limestone-LS) but a more diverse mixture of mineralogy. Some noteworthy observations, particularly in the modulus cross-plots, of using a linear estimation are an underestimation of mineral moduli and an overestimation of critical porosity. The LMrho (Figure 3) and V_p/V_s vs I_p , agrees with the published relationship for mineralogy but also show the shift with burial and mineralogy mixing.

Extending the results using data from offshore New Zealand, Australia and Canada shows how machine learning can be generalized for the estimation of mineralogy along with the estimation of missing acoustic logs required for AVO and Inversion analysis. Finally, the poster provides a comparison against the empirical relationship for V_p , V_s and density.

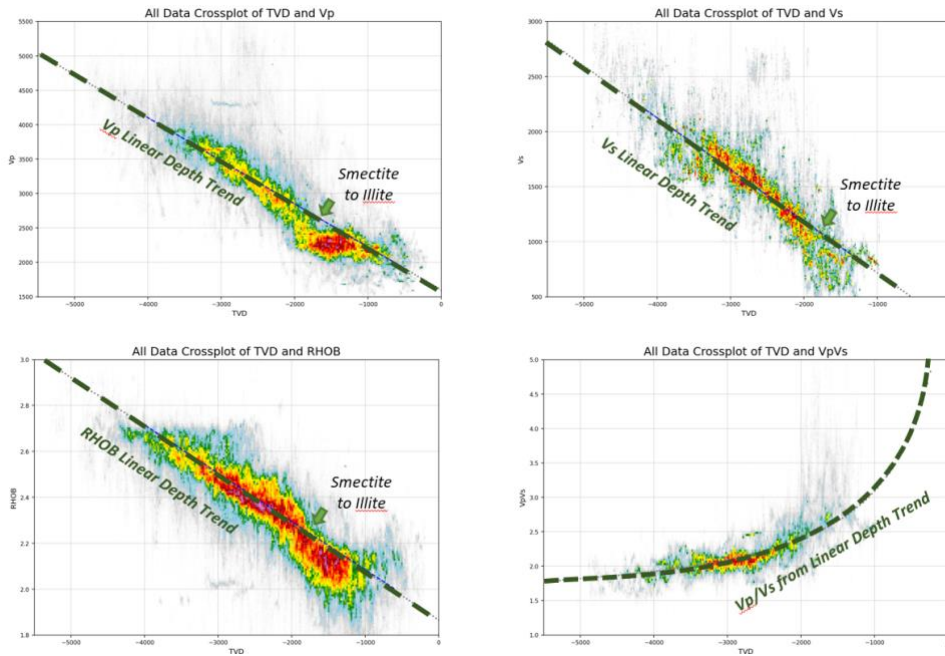


Figure 2: 100% input data plotted against depth, strong discontinuity at -1800 m is assumed to be the location of smectite clay conversion into illite.

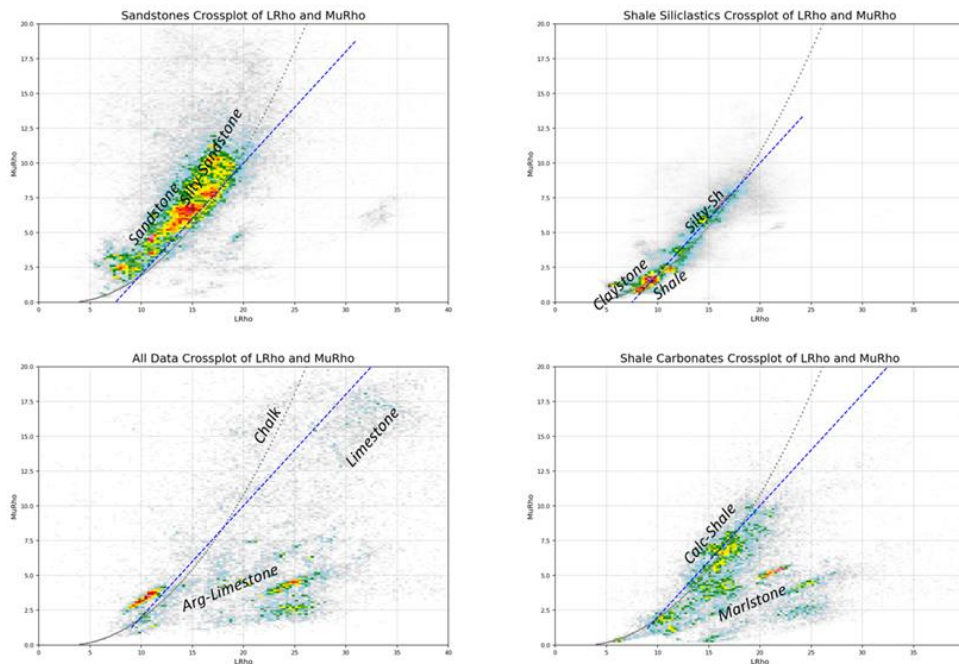


Figure 3: Lambda-Rho vs Mu-Rho for sandstone (upper-left), siliciclastic shales (upper-right), calc-shales (lower-right) and limestone (lower-left) mineralogy. The Grey line from linear Vp, Vs & RHOB fits the 100% data and the blue line linear fits the 100% data.

Conclusions

Machine Learning analysis for mineralogy shows how we can improve over previous approaches using empirical relationships and extend our understanding of mineralogy and burial on the common cross-plots used for seismic analysis. While additional work is required, machine learning has helped provide new insights into the determination of mineralogy from both petrophysical logs and seismic.

Acknowledgements

The authors thank the sponsors of CREWES for their continued support. This work was funded by CREWES industrial sponsors and NSERC (Natural Science and Engineering Research Council of Canada) through the grant CRDPJ 461179-13 and CRDPJ 543578-19 and the financial support from Canada First Research Excellence Fund.

References

- Aki, K., & Richards, P. G. (1980). *Quantitative Seismology*. W. H. Freeman.
- Avseth, P. A., & Odegaard, E. (2004). Well Log and Seismic Data Analysis using Rock Physics Templates. *First Break*, 22, 37-43.
- Avseth, P., Jørstad, A., van Wijngaarden, A. J., & Mavko, G. (2009). Rock physics estimation of cement volume, sorting, and net-to-gross in North Sea sandstones. *The Leading Edge*, 28(1), 98-108.
- Avseth, P., Mukerji, T., Mavko, G., & Dvorkin, J. (2010). Rock-physics diagnostics of depositional texture, diagenetic alterations, and reservoir heterogeneity in high-porosity siliciclastic sediments and rocks—A review of selected models and suggested workflows. *Geophysics*, 75(5), 75A31-75A4.
- Brown, A. R. (1999). Interpretation of 3-dimensional seismic data. *AAPG Memoir*, 42, 341.
- Castagna, J. P., Batzle, M. L., & Eastwood, R. L. (1985). Relationship Between Compressional-Wave and Shear-Wave Velocities in Clastic Silicate Rocks. *Geophysics*, 50, 571-581.
- Castagna, J. P., Batzle, M. L., & Kan, T. K. (1993). Rock physics – The link between rock properties and AVO response: in *Offset-Dependent Reflectivity – Theory and Practice of AVO Analysis*. In J. Castagna, & M. Backus, *Investigations in Geophysics* (pp. 135-171). Tulsa, Oklahoma: Society of Exploration Geophysicists.
- Castagna, J. P., Swan, H. W., & Foster, D. J. (1998). Framework for AVO gradient and intercept interpretation. *Geophysics*, 63, 948-956.
- Connolly, P. (1998). Elastic Impedance. *The Leading Edge*, 18(4), 438.
- Downton, J. E., Collet, O., P, H. D., & Colwell, T. (2020). Theory-Guided Data Science-Based Reservoir Prediction of a North Sea Oil Field. *The Leading Edge*, 742-749.
- Eastwood, R. L., & Castagna, J. P. (1983). Basis for Interpretation of Vs/Vp Ratios in Complex Lithologies. *Proceedings of 24th SPWLA Annual Logging Symposium*.
- Emery, D. J., & Steward, R. R. (2006). Using VP/VS to explore for sandstone reservoirs: well log and synthetic seismograms from the Jeanne d'Arc basin, offshore Newfoundland. *CREWES Research Report*, 18.
- Emery, D. J., Guarido, M., Trad, D. O., & Innanen, K. A. (2021). Lessons Learned, Pitfalls and Feature Engineering for FORCE 2020: Log Facies Classification using Machine Learning. *Geoconvention 2021*.
- Emery, D. J., Guarido, M., & Trad, D. O. (2022). The Pitfalls and Insights of Log Facies Classification using Machine Learning. *SEG Research Workshop: Data Analytics & Machine Learning for Exploration & Production*.
- Emery, D., Guarido, M., Russell, B., & Trad, D. (2022). Machine learnings and lessons learned on improvements to Castagna's mudrock, Gardner's density, and Faust's velocity estimation. *International Meeting for Applied Geoscience & Energy* (p. 4). Houston: SEG/AAPG.

- Faust, L. Y. (1951). Seismic Velocity as a Function of Depth and Geologic Time. *Geophysics*, 16, 192-206.
- Faust, L. Y. (1953). A Velocity Function including Lithologic Variation. *Geophysics*, 18, 271-288.
- FORCE. (2022, February). Results of the FORCE 2020 lithology machine learning competition. Retrieved from <https://www.npd.no/en/force/Previous-events/results-of-the-FORCE-2020-lithology-competition/>
- Gardner, G. H., Garner, L. W., & Gregory, A. R. (1974). Formation velocity and density – The diagnostic basics for stratigraphic traps. *Geophysics*, 39, 770-780.
- Goodway, B. (2001). AVO and Lamé constants for rock parameterization and fluid detection. *CSEG Recorder*, 26(6), 39-60.
- Goodway, W., Chen, T., & Downton, J. (1997). Improved AVO fluid Detection and Lithology Discrimination Using Lamé Petrophysical Parameters. SEG 67th Annual International Meeting, Denver.
- Guarido, M. (2019). Machine Learning Strategies to Perform Facies Classification. *Geoconvention 2019*.
- Guarido, M., Emery, D. J., Macquet, M., T. D., & Innanen, K. A. (2020). The Pitfalls and Insights of Log Facies Classification for a Machine Learning Contest. *CREWES Research Report*, 32, 18.
- Hall, B. (2016). Facies classification using machine learning. *The Leading Edge*, 35(10), 906-909.
- Hall, M., & Hall, B. (2017). Distributed collaborative prediction: Results of the machine learning contest. *The Leading Edge*, 36(3), 267-269.
- Hampson, D. P., Russell, B. H., & Bankhead, B. (2005). Simultaneous inversion of pre-stack seismic data. *SEG Technical Program 2005*.
- Hampson, D., Schuelke, J. S., & Quirein, J. A. (2001). Use of multi-attribute transforms to predict log properties from seismic data. *Geophysics*, 66, 220-231.
- Hoffe, B., Perez, M., & Goodway, W. (2008). AVO interpretation in LMR space: A primer. *Back to Exploration*, 31-34.
- Lee, M. W. (2006). A simple method of predicting S-wave velocity. *Geophysics*, 71(6), 161-164.
- Lindseth, R. O. (1976). Synthetic sonic logs - a process for stratigraphic interpretation. *Geophysics*, 44, 3-26.
- Mavko, G., Mukerji, T., & Dvorkin, J. (1998). *The Rock Physics Handbook: Tools for seismic analysis in porous media*. Cambridge University Press.
- Nur, A., Mavko, G., Dvorkin, J., & Gal, D. (1995). Critical porosity: the key to relating physical properties to porosity in rocks. 65th Annual International Meeting (p. 878). Society of Exploration Geophysics.
- Ostrander, W. J. (1984). Plane-wave reflection coefficients for gas sands at nonnormal angles of incidence. *Geophysics*, 49, 1637-1648.
- Russell, B., & Hampson, D. (1991). Comparison of post-stack seismic inversion methods. *SEG Technical Program Expanded Abstracts 1991*, 876-878.
- Russell, B., & Lines, L. (2013). A Gassmann-consistent rock physics template. *CSEG Recorder*.
- Russell, B., Hampson, D., Schuelke, J., & Quirein, J. (1997). Multiattribute seismic analysis. *The Leading Edge*, 16, 1439-1443.
- Shuey, R. T. (1985). A simplification of the Zoeppritz equations. *Geophysics*, 50(4), 609-614.
- Tanner, M. T., & Sheriff, R. E. (1977). Application of amplitude frequency and other attributes to stratigraphic and hydrocarbon determination. In C. E. Payton, *Seismic stratigraphy - applications to hydrocarbon exploration* (Vol. 26, pp. 301-327). Tulsa: AAPG Memoir.
- Tatham, R. H. (1982). Vp/Vs and Lithology. *Geophysics*, 47, 336-344.